AGU PUBLICATIONS

Geophysical Research Letters

RESEARCH LETTER
10.1002/2017GL074430

Key Points:
- Size distributions spanning cloud droplets to drizzle have been measured with the Holographic Detector for Clouds (HOLODEC)
- Droplets in the size range between condensation and collision growth, which are seldom measured, contribute strongly to cloud properties
- Measurements of the condensation-collision transition droplets brings in-situ and satellite measurements in closer agreement

Supporting Information:
- Supporting Information S1

Correspondence to:
R. A. Shaw,
rashaw@mtu.edu

Citation:
Glienke, S., A. Kostinski, J. Fugal, R. A. Shaw, S. Borrmann, and J. Stith (2017), Cloud droplets to drizzle: Contribution of transition drops to microphysical and optical properties of marine stratocumulus clouds, *Geophys. Res. Lett.*, *44*, 8002–8010, doi:10.1002/2017GL074430.

Received 2 JUN 2017
Accepted 20 JUL 2017
Accepted article online 26 JUL 2017
Published online 11 AUG 2017

Cloud droplets to drizzle: Contribution of transition drops to microphysical and optical properties of marine stratocumulus clouds

S. Glienke[1,2], A. Kostinski[2], J. Fugal[1,3], R. A. Shaw[2], S. Borrmann[1,3], and J. Stith[4]

[1]Johannes Gutenberg University, Mainz, Germany, [2]Michigan Technological University, Houghton, Michigan, USA, [3]Max Planck Institute for Chemistry, Mainz, Germany, [4]National Center for Atmospheric Research, Boulder, Colorado, USA

Abstract Aircraft measurements of the ubiquitous marine stratocumulus cloud type, with over 3000 km of in situ data from the Pacific during the Cloud System Evolution in the Trades experiment, show the ability of the Holographic Detector for Clouds (HOLODEC) instrument to smoothly interpolate the small and large droplet data collected with Cloud Droplet Probe and 2DC instruments. The combined, comprehensive instrument suite reveals a surprisingly large contribution in the predrizzle size range of 40–80 μm (transition droplets, or drizzlets), a range typically not measured and assumed to reside in a condensation-to-collision minimum between cloud droplet and drizzle modes. Besides shedding light on the onset of collision coalescence, drizzlets are essential contributors to optical and chemical properties because of a substantial contribution to the total surface area. When adjusted to match spatial resolution of spaceborne remote sensing, the missing drizzlets bring in situ measurements to closer agreement with satellite observations.

1. Introduction

The enduring puzzle in warm cloud microphysics is the initiation of precipitation, or the transition from growth by diffusion to that by coalescence; in particular, at what size range the transition occurs. It has long been believed [*Kessler*, 1969] that coalescence only becomes efficient for cloud droplet diameters greater than approximately 40 μm, the notion behind the now ubiquitous term "autoconversion" [e.g., *Cotton*, 1972; *Beheng*, 1994; *Liu et al.*, 2005]. Several other reasons point to 40 μm and beyond as a critical size range. For example, how well is the cloud base defined in lidar or radar time-height profiles in drizzling stratocumulus? Drizzle is recognizable as fall streaks: a 40 μm diameter drop falls approximately 100 m in a typical observation time of an hour, so this can serve as a lower bound. Consistent with that picture, drizzle is etymologically derived from "fall" or "drip." An adjacent criterion for defining drizzle is for its fall speed to exceed typical fluctuations in vertical velocity in the cloud (w_{rms}). For a reasonable range of stratocumulus $w_{rms} = 0.1$ to 1 m s^{-1}, the corresponding diameters are approximately 50 to 250 μm. In other words, droplets in this size range are expected to have noticeable drift. Surveying the literature shows that definitions of drizzle vary greatly but usually set the lower limit at diameters about 100 μm. Wood defines it as volume diameter between 60 and 200 μm [*Wood*, 2012], and the Glossary of Meteorology suggests simply precipitation with diameter less than 500 μm [*American Meteorological Society,* 2017]. The arguments above would point to diameters as low as 40 μm experiencing significant drift and likely being grown by coalescence, which are the characteristics of drizzle. Therefore, throughout this manuscript we shall refer to drops in this predrizzle 40 to 80 μm transition size range as drizzlets as a shorthand for small drizzle drops.

Drizzlets are the size range in which coalescence is just initiated, and need not be rigidly defined. We select the 40–80 μm range based on the following, physical reasoning. The familiar Hocking limit is 38 μm and therefore is close to the onset diameter for efficient coalescence [*Hocking and Jonas*, 1970]. Doubling the diameter from 40 to 80 μm is achieved by increasing mass by 2^3, or eight coalescence events. Thus, the drizzlet size range contains drops grown by small, integer number of coalescence events and therefore is subject to pronounced fluctuations [*Kostinski and Shaw*, 2005] where the "stochastic" coagulation equation may not be adequate (i.e., the stochastic coagulation is in fact deterministic and does not account for discrete, "shot noise" fluctuations). Beyond this range, continuous coalescence is a reasonable approximation. Parcel models based on the coagulation equation predict a substantial gap

between cloud droplets and drizzle drops, which we could refer to loosely as the condensation-to-collision growth gap, or autoconversion gap [*Berry and Reinhardt*, 1974; *Flossmann et al*., 1985; *Tzivion (Tzitzvashvili) et al*., 1987; *Seeβelberg et al*., 1996]. Indeed, bimodality in the mass-versus-size distribution is widely considered the fingerprint of coalescence, so much so that it has become textbook material [e.g., *Cotton and Anthes*, 1989, Figure 4.3]. Yet measurements that clearly identify the condensation-to-collision growth gap in natural clouds are difficult to find.

To that end, our objective is to explore the previously neglected drizzlet range with a single instrument capable of measuring from cloud droplet to drizzle sizes. Measurements of the size range 40 to 80 μm have been sparse largely for instrumental reasons. Reliable instruments have existed primarily for measuring cloud droplets (mostly based on single-particle light scattering, such as the Forward Scattering Spectrometer Probe and Cloud Droplet Probe (CDP)) and for drizzle (mostly based on projected area, such as the 2DC optical array probe). Projected-area instruments are able to measure smaller diameters, but large uncertainty in the depth of field makes estimation of concentration troublesome. In practice, concentrations derived from projected-area instruments for droplets of diameter less than about 100 μm are problematic due to the difficulties in obtaining an accurate depth of field for the imaged particles. Whatever lower size range is used, one is still left with the challenge of splicing together two measurements of the size distribution that meet in the drizzlet range. The measurements of collision-coalescence initiators by *Small and Chuang* [2008] are a notable exception, providing a similar context as this paper, but for cumulus clouds. In this paper we analyze data from the Holographic Detector for Clouds (HOLODEC), which measures from a lower diameter of approximately 6 μm to an upper limit above 500 μm (for a size distribution, the upper limit also depends on drop concentration and sampled cloud volume). We chose to examine data from drizzling marine stratocumulus clouds because of their near permanence over vast areas of the globe. This prevalence suggests their importance for albedo and therefore global energy balance. To that end, and with the condensation-to-collision growth gap in mind, we ask, how do the drizzlets contribute to drop number concentration, to cloud optical properties (related to the total drop surface area), and to liquid water content (total drop volume)?

2. Experiment and Methods

2.1. Overview of CSET

During the Cloud System Evolution of the Trades (CSET) project in July and August 2015, 16 research flights off the coast of California were made in order to measure marine stratocumulus cloud properties and to explore their evolution. For this purpose, the NSF/National Center for Atmospheric Research (NCAR) Gulfstream-V High-performance Instrumented Airborne Platform for Environmental Research (GV HIAPER) aircraft [*UCAR/NCAR-Earth Observing Laboratory*, 2005] was fitted with both in situ and remote sensing measurement instruments and flew pairs of flights between California and Hawaii [*UCAR/NCAR-Earth Observing Laboratory*, 2017].

The specific case considered here is from several cloud passes during flight RF07 on 19 July 2015, where the aircraft dipped repeatedly into the same cloud system at different places at about 20:45–20:54 UTC (138.1–137.3 W and 26.7–26.3 N). The cloud system was about half way between California and Hawaii in an area with mostly open mesoscale cellular convective clouds, and it was nearly 100 km in length. The cloud thickness varied across the system, but according to RADAR and lidar on the GV and satellite imagery, the system is connected.

2.2. Cloud Microphysical Data and HOLODEC

In CSET several instruments for in situ cloud measurements were deployed. The Cloud Droplet Probe (CDP) measures the scattering of light by a particle and can detect droplet diameters in the range 2–50 μm. Due to the fact that it measures one particle at a time, the sample volume is continuous, but for a reliable size distribution all droplets from 1 s of flight have to be analyzed; at a flight speed of 150 m s^{-1} this gives a long, thin sample volume of approximate dimensions $0.02 \times 0.2 \times 15000$ cm^3 each second [e.g., *Lance et al*., 2010]. Also on board was a 2DC optical array probe for measurement of drizzle drops. Optical array probes also measure individual particles at a time; when a particle enters the sample area, it will obscure diodes and, in

combination with the flight speed, the size of the particle can be determined. The 2DC data for diameters of 100 μm and above are used in this study, due to the depth-of-field uncertainties already mentioned.

Another cloud instrument on CSET was the Holographic Detector of Clouds (HOLODEC). Rather than recording cloud droplets one by one, HOLODEC takes a snapshot of a localized sample volume of 13 cm^3 of air with all droplets inside (one hologram) at a rate of 3.3 Hz [*Fugal and Shaw*, 2009; *Spuler and Fugal*, 2011]. This has the advantage that one can look at the local properties of the cloud [*Beals et al*., 2015], albeit with gaps between individual sample volumes. HOLODEC is able to detect all drop sizes larger than about 6 μm, with sampling on the large-drop end limited by the number concentration and sampled volume. This enables the measurement of a large range of sizes by one instrument without the difficulty of comparing results from different instruments, where uncertainties are greatest in the overlapping size range, if they overlap at all. Roughly the size range of 40–100 μm often has the least certainty in measurements, due to the depth of field uncertainties and associated uncertainty in sample volume mentioned earlier. HOLODEC performs well in this regard because of its well-defined sample volume and because the drops are large enough to be detected and sized confidently and still present in high enough concentrations to yield good counting statistics.

In order to process the HOLODEC data from CSET, 455,980 holograms had to be reconstructed, with each hologram reconstruction requiring computation of 1600 planes along the optical axis, and then searched for particles. This job required substantial high-performance computing support [e.g., *Computational and Information Systems Laboratory*, 2012], for a total of about 2.8 million core compute hours. After reconstruction, the candidate droplets have to be classified in order to separate real droplets from noise artifacts and to determine droplet size and three-dimensional spatial position. For the RF07 analysis this has been accomplished with a combination of machine and supervised analysis in order to achieve the lowest false detection rates. Results from all other flights were analyzed with unsupervised machine classification; the latter method will have slightly higher false detection rates but comparing to other instruments as well as comparing to supervised-classification data in several sections shows that this effect is small. This is the first time all data taken during an entire field project such as CSET with an airborne holographic instrument such as HOLODEC has been fully reconstructed and analyzed for scientific use.

2.3. Satellite Data

The region that was sampled during CSET was covered for all times by the Geostationary Operational Environmental Satellite GOES 15. The larger cloud system sampled by the GV during RF07 was resolved by GOES 15 with 37 pixels with a spatial resolution of about 10 km by 10 km. This means a comparison between the two very different methods, in situ and remote sensing, is possible, but has the typical challenges associated with matching scales. The aircraft only penetrated the cloud system in four distinct places, so the assumption of statistical homogeneity is inherent in the comparison. GOES 15 cloud effective diameters were retrieved using the NASA Langley Satellite Cloud and Radiative Property retrieval System, described by *Minnis et al*. [2008, 2016].

3. Results

Our results in Figure 1 show that contrary to the notion of the condensation-to-collision growth gap, no gap is observed. Furthermore, the drizzlets make a substantial contribution to the surface area and volume of the cloud. Two examples have been chosen, both from the same cloud system, with one vertical transect through a weakly drizzling cloud (Figure 1, left) and one vertical transect through a strongly drizzling cloud (Figure 1, right). Consider, for example, the strongly drizzling case of Figure 1 (right) where the drizzlets account for only 9% of the total population, yet contribute 31% (3.5 times increase) to the surface area and 35% the volume. Thus, one expects an important contribution to the optical properties such as the optical depth (τ) and liquid water path (L) as well as their inverse ratio, the effective diameter (d_{eff}). In the weakly drizzling case as well (Figure 1, left), the drizzlets make up 16% of the total population but supply 36% of the surface area (hence, optical depth) and nearly half of total liquid water content (hence, liquid water path). It is worth noting that this is not a unique case, and similar results are observed throughout the CSET data set. Even when a hint of bimodality is observed, the contributions of drizzlets to surface area and volume are still substantial (see supporting information, Figure S1).

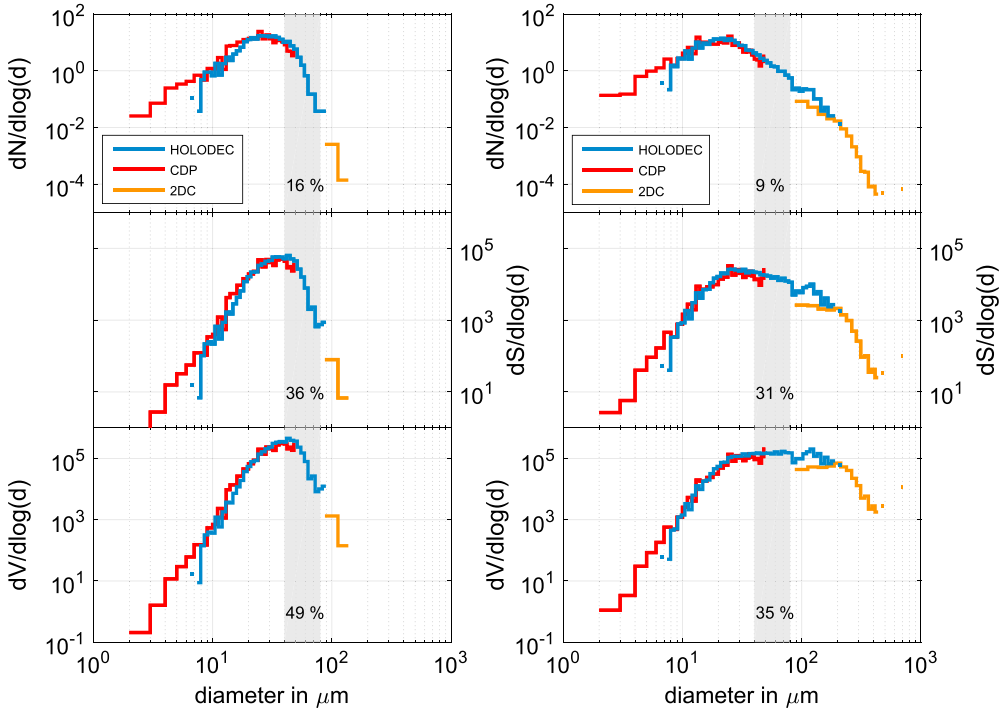

Figure 1. Comprehensive and mutually consistent droplet size coverage shows unimodal size distributions, with drizzlets (gray band) contributing substantially to surface area and volume. Measured (CDP, Holodec, and the 2DC) size distributions of droplets from two, shallow-slope flights through (left) weakly drizzling and (right) drizzling stratocumulus cloud. The panels are histograms of (top) number (N), (middle) surface area (S), and (bottom) volume (V). The gray band covers the predrizzle (drizzlet) size range. The percentage in each panel denotes the fractional contribution of drizzlets to N, S, and V, measured with HOLODEC. The suite of three instruments spans 2.5 orders of magnitude in droplet diameter, with matching junctions of the distributions. Serendipitously, the HOLODEC appears perfectly suited to fill in the distributions in the drizzlet range. We note that with HOLODEC removed there could be an illusion of bimodality, supported by spurious agreement with expectations from models. Rather than being bimodal, with a dip in the gray band (signature of coalescence onset), the surface and volume distributions show substantial contribution of the drizzlets. This is true both for the cloud on the verge of drizzling (Figure 1, left) and even more so for the strongly drizzling cloud (Figure 1, right). Note that for the strongly drizzling cloud, the equal contributions to volume throughout the gray band and beyond (nearly a factor of 10 in droplet diameter). Recall that growth by coalescence decreases total surface area but preserves volume, while growth by diffusion increases both. Figure 1 (left) corresponds to approximately 20 s (i.e. ~3 km) of sampled cloud and the right panel corresponds to approximately 1 min (i.e., ~9 km) of sampled cloud (although the latter contains some gaps interspersed).

While in Figure 1 only two cloud transects were examined, in Figure 2 we display data from 14 flights over the 1 month time span of the CSET project, which include more than 3000 km of cloud sampling. Of the 4552 5 s cloud segments, approximately 40% are devoid of drizzlets and are not displayed in the figure because of the logarithmic scale. The remaining 60% of 5 s segments (2756 in total) each contain one or more drizzlets. A 5 s segment includes 17 holograms, and therefore a total sampled volume of approximately 221 cm^3. Hence, drizzlets are a common feature of these clouds and, as shown in the figure, when they are present, they contribute prominently to surface area, especially in cleaner clouds. The two-dimensional histogram shows an anticorrelation between the drizzlet contribution to surface area and the total number concentration as indicated by the negative slope. Furthermore, at least two populations or modes of drizzlet contribution to surface area are observed in the joint histogram in Figure 2. The high-occurrence (yellow) region in the upper left corresponds to clouds with exceptionally low droplet concentrations of just a few droplets per cubic centimeter (when averaged over 5 s, approximately 0.75 km), but with drizzlets contributing up to half of the total surface area of the cloud. It might be assumed that these drizzlet-dominated clouds are the remnants of rained-out clouds, but the same data set (see supporting information, Figure S2) reveals that drizzlet contribution to cloud surface area shows no significant preference for total liquid water content (where liquid water content here is determined from the HOLODEC measurements for consistency). Parcels with peak liquid water content are observed to exist with and without drizzlets. In other words, the

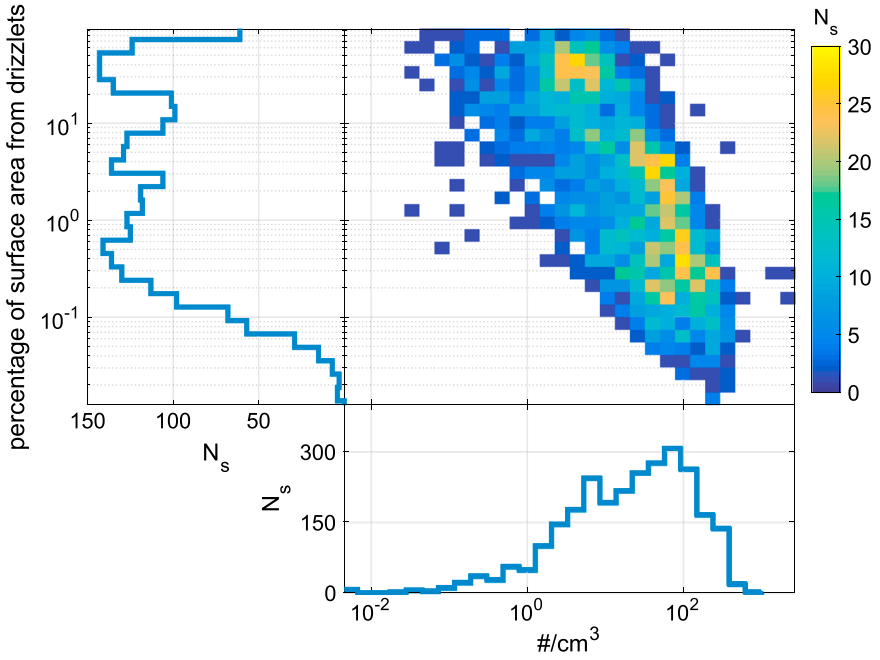

Figure 2. Examination of all in-cloud data from all 14 flights with HOLODEC on board (dates: 7 July to 12 August 2015), spanning about 3000 km within clouds, demonstrates that drizzlets occur throughout and contribute significantly to the optical properties of these marine stratocumuli. The plot is a joint histogram of droplet number concentration and the percentage of cloud surface area contributed by drizzlets (with individual histograms of the two quantities also shown). N_s is the number of 5 s samples. The joint histogram shows a nearly continuous maximum with negative slope (yellow pixels), signifying anticorrelation between the drizzlet contribution to surface area and the total number concentration. In other words, drizzlets are predominant in cleaner clouds (only about five droplets per cubic centimeter). Note also the distinct classes (yellow blobs) in the joint pdf: drizzlets in the upper "low-concentration" blob contributing about half of the entire surface area while the lower "higher-concentration" one hardly containing any drizzlets.

drizzlet-dominated cloud population observed in Figure 2 contains regions with high liquid water content and can therefore be considered extremely clean clouds that have not yet been depleted by rainout. The primary microphysical distinction is therefore the drizzlet concentration, as well as the enhanced variability in liquid water content observed for the drizzlet-dominated clouds (see Figure S2). In clouds with peak liquid water content, which is approximately independent of drizzlet contribution, it is therefore clear that drizzlet-dominated clouds have low droplet concentrations.

These results suggest that drizzlets occur frequently in marine stratocumulus clouds and that they make a substantial contribution to the optical properties of these "global reflectors." We can extend this analysis by calculating the effective diameter, defined as

$$d_{\text{eff}} = \frac{\overline{d^3}}{\overline{d^2}}$$

and comparing it to the retrieved droplet effective diameter from satellite measurements taken at the same time. Drizzlets are found in multiple flights, throughout the 1 month measurement period, but for our purposes we select the case shown in Figure 1. The GOES effective diameter estimates are shown in Figure 3. A contrasting case with much smaller droplets from RF02 is shown in Figure S3. It is immediately striking that effective diameters greater than 20 μm are observed over large portions of the eastern Pacific (yellow, orange, and red pixels), suggesting that the cloud optical properties indeed are dominated by droplets within the transition drop (drizzlet) range. The region of in situ measurements is indicated by the box, and the resulting distribution of effective radius within that region is compared to the distribution obtained from the HOLODEC measurements. The distribution of GOES-retrieved d_{eff} is shown in Figure 3 (right) and has a mean value of 48.2 μm, compared to a mean of 44.4 μm for HOLODEC, and a mean of 46.6 μm for all three in situ instruments (the latter is obtained by using the HOLODEC range between 10 and 100 μm, the CDP droplets below that range due to better detectability, and the 2DC droplets above that range due to the low number

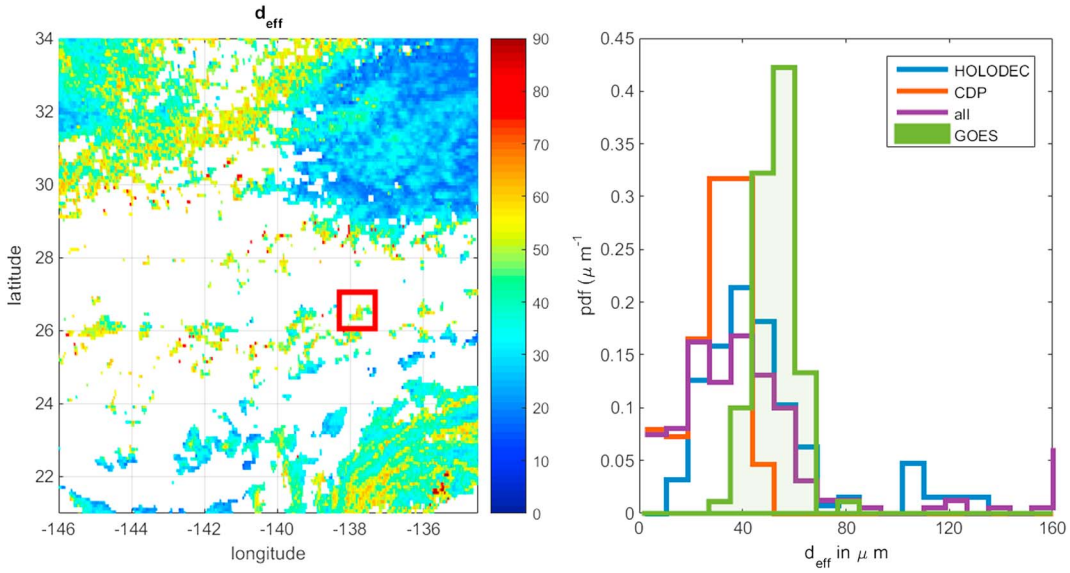

Figure 3. Abundant drizzlets found in aircraft measurements bring estimates of effective diameters closer to the remotely sensed ones. (left) GOES retrieval of the effective diameter in the general vicinity of the flight path (red square) at the time of the satellite image (21 UTC). The flight path linked Hawaii and Northern California. Large fraction of boundary layer clouds in this eastern Pacific region have surprisingly large effective diameters (up to 80 μm), suggesting essential contribution of drizzlets to total surface area. The GOES mean of the region in the red square is 48 μm and appears ubiquitous within the image. (right) Comparison of effective diameter distributions measured by the comprehensive suite of instruments (color) with GOES retrievals (green shaded). The aircraft measurements have been coarsened to approximate the GOES resolution (~1 km). Note that the oft observed retrieval bias toward larger d_{eff} is greatly reduced (44 μm for HOLODEC versus 48 μm for GOES, whereas 26 μm for CDP). This improvement is largely due to resolving drizzlets in situ.

concentrations). We note in passing that in several cases, the peak of the size distribution is found in the drizzlet range and in the majority of the cases drizzlets contribute largely to the size distribution; therefore, it is more robust to use the data from HOLODEC to bridge between the data from CDP and 2DC rather than a simple mathematical interpolation, which could give large errors particularly on a logarithmic scale. The GOES-retrieved and in situ estimates are all within the drizzlet size range, confirming the dominance of drizzlets for cloud optical properties as well as the large areal coverage of drizzlet-dominated clouds. The retrieved and in situ estimates nearly agree to within the uncertainty of the in situ measurements; the GOES estimates are slightly greater than the in situ measurements, but the bias is considerably less than has been reported before [e.g., *Szczodrak et al.*, 2001; *Painemal and Zuidema*, 2011]. The improved agreement can be directly attributed to the resolved drizzlets: for example, the effective diameter obtained from the CDP alone is 25.8 μm. In other words, while it is not surprising that the CDP alone does not agree, due to its upper measurement limit, the analysis shows that including the 2DC measurements does not significantly improve agreement; it is thus the drizzlet category so often missing from in situ measurements that is necessary for an improved comparison with the satellite data. Further improvement likely depends on details and assumptions related to the retrieval.

4. Discussion

The warm rain problem can be summarized as the competition between two growth mechanisms, condensation versus coalescence. The former conserves number and increases both surface area and volume of the droplet population; the latter conserves volume and decreases both number and surface area. We have investigated the number, surface area, and volume distributions of droplets in marine stratocumulus clouds using a suite of three instruments that span the full range of droplet sizes, from cloud droplets to drizzle. Significantly, the HOLODEC instrument enables droplets in the typical measurement gap to be directly and reliably observed. Besides rarely being measured, these droplets in the "autoconversion" size range are crucial to understanding the competing roles of condensation and coalescence. Because of their expected importance in the transition from condensation to coalescence, we refer to droplets with diameters between 40 and 80 μm as drizzlets. We quantify the contribution of this poorly explored size range to the number,

surface area, and volume of clouds. Examining data on surface area and volume along with number concentration brings additional insight into optical and chemical (surface area-dependent) properties.

Overall, the clouds observed during CSET tend to be nearly drizzling to strongly drizzling, as is typical for closed- and open-cellular convection [*Stevens et al*., 2005; *Wood et al*., 2008; *Feingold et al*., 2010]. The figures illustrate how HOLODEC presents a relatively rare opportunity to resolve the drizzlet drop size range, bridging cloud droplets to drizzle, with a single instrument. The three in situ instruments together therefore offer a glimpse of the full size distribution for clouds with and without drizzle production. We note further that HOLODEC is particularly well suited to the study of cloud optical properties because after the hologram reconstruction, particle size is determined directly from the particle projected area. Therefore, surface area is the most closely related to the fundamental measurement method. And indeed, the effective diameter calculated from the distributions lies in the drizzlet range.

The main observations can be summarized as follows: (1) In contrast to expectations from theory, observations of bimodality and the condensation-to-collision growth gap (or autoconversion gap) were relatively rare in these clean, marine stratocumulus clouds; (2) droplets in the range where condensation growth is expected to transition to the onset of collisional growth, here called drizzlets, are common in these clouds and contribute strongly to surface area and volume of the clouds; (3) effective diameters for many of the marine stratocumulus clouds lie in the drizzlet size range; and (4) the ability to resolve drizzlets using the HOLODEC instrument brings the in situ measurements into much closer agreement with the retrieved effective diameter distribution from GOES.

We can speculate on two possible microphysical mechanisms for the formation of ultraclean, drizzlet-dominated clouds often observed in the CSET data. It is well accepted that in very clean, low-aerosol-concentration environments, the mean cloud droplet size is increased, assuming liquid water content is fixed. As shown above, many of the drizzlet-dominated clouds exhibit liquid water contents similar to clouds without drizzlets. It has already been shown that, indeed, many of the drizzlet-dominated clouds have peak liquid water contents equivalent to the more polluted clouds observed. Can the drizzlets be realistically attributed to condensation growth? Parcel model calculations are often cited as requiring unrealistically long times for growth to diameters greater than approximately 40 μm, and this is especially expected to be true for relatively shallow, marine stratocumulus clouds such as observed in most of CSET. However, the recent study by *Jensen and Nugent* [2017] has shown that if these clouds contain giant cloud condensation nuclei such as those expected from marine sea salt aerosol, the large salt aerosol can grow to drizzle-sized particles even in the relatively weak updraft conditions found in marine stratus (indeed, their study has shown that they can grow even in downdrafts if the salt concentrations are great enough). Thus, future studies that compare the levels of large sea salt particles with drizzlets should help explore this mechanism. A second mechanism may be found in recent laboratory and field work showing that supersaturation fluctuations can be pronounced, and droplet size distribution width greatly enhanced [*Chandrakar et al*., 2016; *Siebert and Shaw*, 2017]. The large fluctuations exist in the clean-cloud limit, when cloud droplet response is slow compared to turbulent correlation time. This has been argued as a mechanism for growth of large droplets capable of initiating the collision-coalescence process, and eventual cloud collapse [*Chandrakar et al.,* 2017]. We consider whether such a mechanism could be operating here. The relevant microphysical time scale for this turbulence-broadening effect [*Chandrakar et al*., 2016] is the phase relaxation time, given by $\tau_{\mathrm{phase}} = \left(2\pi D_v' n \overline{d}\right)^{-1}$, where D_v' is a modified water vapor diffusion coefficient and $\overline{d}$ is the mean droplet diameter, and n is droplet concentration [*Kumar et al*., 2014]. The relevant turbulence time scale is the Lagrangian correlation time for the large-scale mixing and can be roughly estimated from the Eulerian large-eddy correlation time. We have estimated the phase relaxation times for the clouds corresponding to Figures 1 and 3 and find that τ_{phase} varies within the approximate range tens to hundreds of seconds, with the larger values typical of low-droplet-concentration drizzlet clouds. Using the gust probe data, we calculate w_{rms} and the velocity autocorrelation length scale l and combine them to get a turbulence correlation time of order $\tau_{\mathrm{turb}} \sim l/w_{\mathrm{rms}} \sim 10^2$ s. This suggests that drizzlet-dominated clouds exhibit $\tau_{\mathrm{phase}} \sim \tau_{\mathrm{turb}}$ and therefore reside in the vicinity of the transition between the usual polluted cloud (fast microphysics) limit of $\tau_{\mathrm{phase}} \ll \tau_{\mathrm{turb}}$ and the clean cloud (slow microphysics) limit of $\tau_{\mathrm{phase}} \gg \tau_{\mathrm{turb}}$. Thus, the data are consistent with the following picture: the cleansing that leads to very low cloud condensation nucleus concentrations [*Wood*, 2006; *Goren and Rosenfeld*, 2015], together

with the weak turbulence typical of marine stratocumulus clouds, allows cloud droplet concentrations to become so low that turbulent fluctuations of supersaturation can dominate the droplet growth and produce very large droplets even in the drizzlet range through condensation alone [*Chandrakar et al.*, 2017]. As mentioned, these estimates are for the drizzlet-dominated clouds shown in Figures 1 and 3, providing only initial, localized insights. Further study will be required to determine the extent to which the above mechanisms are operating in clouds such as in CSET; this work clearly demonstrates that such studies will require suitable instrumentation for sampling in the drizzlet size range.

Acknowledgments

This research was supported by U.S. National Science Foundation (NSF) grants AGS-1623429 and AGS-1639868. The National Center for Atmospheric Research is sponsored by NSF. We are grateful to the CSET science team (B. Albrecht, C. Bretherton, R. Wood, and P. Zuidema) and the NCAR Earth Observing Laboratory and its Research Aviation Facility for the project organization and implementation. We thank A. Shaw for helpful discussions on the data interpretation. The GOES 15 image and effective radii were obtained from P. Minnis, R. Palikonda, and the NASA Langley Cloud and Radiation Research Group, https://satcorps.larc.nasa.gov/cset. Hologram reconstruction was performed on the following systems, and we acknowledge the support from those facilities, both in computing time and technical assistance: the Portage/Superior computing system at Michigan Technological University (superior.research.mtu.edu), the supercomputer Mogon at Johannes Gutenberg University Mainz (hpc.uni-mainz.de), and Yellowstone (ark:/85065/d7wd3xhc) provided by NCAR's Computational and Information Systems Laboratory, sponsored by NSF. We acknowledge the support of the HoloSuite software team for their contributions to the hologram processing software. Part of this research was carried out while S. Glienke was a visiting scientist at NCAR, supported by the Advanced Study Program. Data used in the study are available from the CSET data archive hosted by NCAR: http://data.eol.ucar.edu/master_list/?project=CSET.

References

American Meteorological Society, cited 2017: "Drizzle". Glossary of Meteorology. [Available online at http://glossary.ametsoc.org/wiki/Drizzle.]

Beals, M. J., J. P. Fugal, R. A. Shaw, J. Lu, S. M. Spuler, and J. L. Stith (2015), Holographic measurements of inhomogeneous cloud mixing at the centimeter scale, *Science*, *350*(6256), 87–90, doi:10.1126/science.aab0751.

Beheng, K. D. (1994), A parameterization of warm cloud microphysical conversion processes, *Atmos. Res.*, *33*(1–4), 193–206, doi:10.1016/0169-8095(94)90020-5.

Berry, E. X., and R. L. Reinhardt (1974), An analysis of cloud drop growth by collection Part II. Single initial distributions, *J. Atmos. Sci.*, *31*(7), 1825–1831.

Chandrakar, K. K., W. Cantrell, K. Chang, D. Ciochetto, D. Niedermeier, M. Ovchinnikov, R. A. Shaw, and F. Yang (2016), Aerosol indirect effect from turbulence-induced broadening of cloud-droplet size distributions, *Proc. Natl. Acad. Sci. U.S.A.*, *113*(50), 14,243–14,248, doi:10.1073/pnas.1612686113.

Chandrakar, K. K., W. Cantrell, D. Ciochetto, S. Karki, G. Kinney, and R. A. Shaw (2017), Aerosol removal and cloud collapse accelerated by supersaturation fluctuations in turbulence, *Geophys. Res. Lett.*, *44*, 4359–4367, doi:10.1002/2017GL072762.

Computational and Information Systems Laboratory (2012) *Yellowstone: IBM iDataPlex System (Univ. Community Computing)*, Natl. Cent. for Atmos. Res., Boulder, Colo. [Available at http://n2t.net/ark:/85065/d7wd3xhc.]

Cotton, W. R. (1972), Numerical simulation of precipitation development in supercooled cumuli—Part I, *Mon. Weather Rev.*, *100*(11), 757–763.

Cotton, W. R., and R. A. Anthes (1989), *Storm and Cloud Dynamics*, *International Geophysics Series*, edited by W. R. Cotton and R. A. Anthes, Academic Press, San Diego, Calif.

Feingold, G., I. Koren, H. Wang, H. Xue, and W. A. Brewer (2010), Precipitation-generated oscillations in open cellular cloud fields, *Nature*, *466*(7308), 849–852, doi:10.1038/nature09314.

Flossmann, A. I., W. D. Hall, and H. R. Pruppacher (1985), A theoretical study of the wet removal of atmospheric pollutants. Part I: The redistribution of aerosol particles captured through nucleation and impaction scavenging by growing cloud drops, *J. Atmos. Sci.*, *42*(6), 583–606, doi:10.1175/1520-0469(1985)042<0583:ATSOTW>2.0.CO;2.

Fugal, J. P., and R. A. Shaw (2009), Cloud particle size distributions measured with an airborne digital in-line holographic instrument, *Atmos. Meas. Tech. Discuss.*, *2*, 659–688, doi:10.5194/amtd-2-659-2009.

Goren, T., and D. Rosenfeld (2015), Extensive closed cell marine stratocumulus downwind of Europe—A large aerosol cloud mediated radiative effect or forcing?, *J. Geophys. Res. Atmos.*, *120*, 6098–6116, doi:10.1002/2015JD023176.

Hocking, L. M., and P. R. Jonas (1970), The collision efficiency of small drops, *Q. J. R. Meteorol. Soc.*, *96*(410), 722–729, doi:10.1002/qj.49709641013.

Jensen, J. B., and A. D. Nugent (2017), Condensational growth of drops formed on giant sea-salt aerosol particles, *J. Atmos. Sci.*, *74*(3), 679–697, doi:10.1175/JAS-D-15-0370.1.

Kessler, E. (1969), On the distribution and continuity of water substance in atmospheric circulations, in *On the Distribution and Continuity of Water Substance in Atmospheric Circulations*, pp. 1–84, Am. Meteorol. Soc., Boston, Mass.

Kostinski, A. B., and R. A. Shaw (2005), Fluctuations and luck in droplet growth by coalescence, *Bull. Am. Meteorol. Soc.*, *86*(2), 235–244, doi:10.1175/BAMS-86-2-235.

Kumar, B., J. Schumacher, and R. A. Shaw (2014), Lagrangian mixing dynamics at the cloudy–clear air interface, *J. Atmos. Sci.*, *71*(7), 2564–2580, doi:10.1175/JAS-D-13-0294.1.

Lance, S., C. A. Brock, D. Rogers, and J. A. Gordon (2010), Water droplet calibration of the cloud droplet probe (CDP) and in-flight performance in liquid, ice and mixed-phase clouds during ARCPAC, *Atmos. Meas. Tech.*, *3*(6), 1683–1706, doi:10.5194/amt-3-1683-2010.

Liu, Y., P. H. Daum, and R. L. McGraw (2005), Size truncation effect, threshold behavior, and a new type of autoconversion parameterization, *Geophys. Res. Lett.*, *32*, L11811, doi:10.1029/2005GL022636.

Minnis, P., et al. (2008), Near-real time cloud retrievals from operational and research meteorological satellites, in *Proc. SPIE 7107, Remote Sensing of Clouds and the Atmosphere*, edited by R. H. Picard et al., p. 710703, doi:10.1117/12.800344.

Minnis, P., K. Bedka, Q. Trepte, C. R. Yost, S. T. Bedka, B. Scarino, K. Khlopenkov, and M. M. Khaiyer (2016), A consistent long-term cloud and clear-sky radiation property dataset from the Advanced Very High Resolution Radiometer (AVHRR), CDR Program Document CDRP-ATBD-0826.

Painemal, D., and P. Zuidema (2011), Assessment of MODIS cloud effective radius and optical thickness retrievals over the Southeast Pacific with VOCALS-REx in situ measurements, *J. Geophys. Res.*, *116*, D24206, doi:10.1029/2011JD016155.

Seeβelberg, M., T. Trautmann, and M. Thorn (1996), Stochastic simulations as a benchmark for mathematical methods solving the coalescence equation, *Atmos. Res.*, *40*(1), 33–48, doi:10.1016/0169-8095(95)00024-0.

Siebert, H., and R. A. Shaw (2017), Supersaturation fluctuations during the early stage of cumulus formation, *J. Atmos. Sci.*, *74*(4), 975–988, doi:10.1175/JAS-D-16-0115.1.

Small, J. D., and P. Y. Chuang (2008), New observations of precipitation initiation in warm cumulus clouds, *J. Atmos. Sci.*, *65*(9), 2972–2982, doi:10.1175/2008JAS2600.1.

Spuler, S. M., and J. P. Fugal (2011), Design of an in-line, digital holographic imaging system for airborne measurement of clouds, *Appl. Opt.*, *50*(10), 1405–1412, doi:10.1364/AO.50.001405.

Stevens, B., G. Vali, K. Comstock, R. Wood, M. C. Van Zanten, P. H. Austin, C. S. Bretherton, and D. H. Lenschow (2005), Pockets of open cells and drizzle in marine stratocumulus, *Bull. Am. Meteorol. Soc.*, *86*(1), 51–57, doi:10.1175/BAMS-86-1-51.

Szczodrak, M., P. H. Austin, and P. B. Krummel (2001), Variability of optical depth and effective radius in marine stratocumulus clouds, *J. Atmos. Sci.*, *58*(19), 2912–2926, doi:10.1175/1520-0469(2001)058<2912:VOODAE>2.0.CO;2.

Tzivion (Tzitzvashvili), S., G. Feingold, and Z. Levin (1987), An efficient numerical solution to the stochastic collection equation, *J. Atmos. Sci.*, *44*(21), 3139–3149, doi:10.1175/1520-0469(1987)044<3139:AENSTT>2.0.CO;2.

UCAR/NCAR-Earth Observing Laboratory (2005), NSF/NCAR GV HIAPER aircraft, UCAR/NCAR-Earth Observing Laboratory, doi:10.5065/D6DR2SJP.

UCAR/NCAR-Earth Observing Laboratory (2017), Low Rate (LRT-1 sps) Navigation, State Parameter, and Microphysics Flight-Level Data, Version 2.0. *UCAR/NCAR-Earth Observing Laboratory*, doi:10.5065/D65Q4T96.

Wood, R. (2006), Rate of loss of cloud droplets by coalescence in warm clouds, *J. Geophys. Res.*, *111*, D21205, doi:10.1029/2006JD007553.

Wood, R. (2012), Stratocumulus clouds, *Mon. Weather Rev.*, *140*(8), 2373–2423, doi:10.1175/MWR-D-11-00121.1.

Wood, R., K. K. Comstock, C. S. Bretherton, C. Cornish, J. Tomlinson, D. R. Collins, and C. Fairall (2008), Open cellular structure in marine stratocumulus sheets, *J. Geophys. Res.*, *113*, D12207, doi:10.1029/2007JD009371.